Journal of Catalysis **196,** 180–189 (2000)
doi:10.1006/jcat.2000.3013, available online at http://www.idealibrary.com on IDEAL®

Sulfidation and Thiophene Hydrodesulfurization Activity of Nickel Tungsten Sulfide Model Catalysts, Prepared without and with Chelating Agents

G. Kishan, L. Coulier, V. H. J. de Beer, J. A. R. van Veen, and J. W. Niemantsverdriet[1]

Schuit Institute of Catalysis, Eindhoven University of Technology, 5600 MB Eindhoven, The Netherlands

Received June 2, 2000; revised July 18, 2000; accepted July 18, 2000

Silica-supported NiWS catalysts with a high activity for thiophene hydrodesulfurization are obtained when chelating agents such as 1,2-cyclohexanediamine-*N*,*N*,*N*′,*N*′-tetraacetic acid (CyDTA), ethylenediaminetetraacetic acid, or nitrilotriacetic acid are added in the impregnation stage. X-ray photoelectron spectroscopy has been used to follow the state of Ni and W during the temperature programmed sulfidation of Ni–W model catalysts prepared with and without chelating agents on planar SiO_2 films on silicon substrates. Fully sulfided catalysts have been tested in thiophene hydrodesulfurization. The activity increases with increasing Ni content and reaches a plateau at a Ni : W atomic ratio of 0.66. In NiW catalysts prepared without additives the sulfidation of Ni precedes that of W. However, Ni sulfide formed at low temperatures changes its structure at high temperatures where WS_2 is present, as indicated by the Ni XPS binding energy, which we tentatively attribute to redispersion of sulfidic Ni over WS_2. Chelating agents stabilize Ni against sulfide formation at low temperature, the effect being strongest when CyDTA is applied. CyDTA retards the sulfidation of Ni to temperatures where all W has already been sulfided. This complete reversal in the order in which the two elements convert to sulfides is seen as the key step in preparing highly active NiWS HDS catalysts. © 2000 Academic Press

Key Words: **model catalyst; sulfidation; XPS; nickel; tungsten; silica; hydrodesulfurization; chelating ligands; thiophene.**

INTRODUCTION

The production of low-sulfur diesel fuels is currently an important topic in oil refineries due to more stringent environmental legislation (1). Hydrodesulfurization (HDS) of refinery streams is carried out with catalysts consisting of Mo promoted with Ni or Co, or W promoted with Ni, all in the sulfided state (2–5). In the preparation, sulfidation of the oxidic precursors in a mixture of H_2S/H_2 or in the sulfur-containing hydrocarbon feed is an essential step. While sulfidation of supported oxidic Mo, CoMo, and NiMo catalysts has received considerable attention (2–12), much less is known about the sulfidation of W-based catalysts. As NiW-sulfide catalysts are becoming increasingly important for deep HDS, more detailed knowledge about their preparation chemistry is desirable.

W and Mo exhibit clearly different behavior with respect to sulfidation. Scheffer *et al.* (3) and Breysse *et al.* (12) showed that NiW/Al_2O_3 catalysts are much more difficult to sulfide than their Mo-based counterparts. Reinhoudt *et al.* (13) reported that complete sulfidation of W resulted in the highest thiophene HDS activity (tested in gas phase), while the highest dibenzothiophene HDS activity (tested in trickle flow) was found when the sulfidation of W was incomplete.

For CoMo or NiMo supported on Al_2O_3 or SiO_2 a fairly complete picture of the active phases exists. These consist of Co or Ni atoms on the edges of MoS_2 slabs and are commonly referred to as CoMoS and NiMoS phases (2, 4, 5, 14–20). An extended X-ray absorption fine structure (EXAFS) study by Louwers and Prins (21) on carbon-supported NiW catalysts provides evidence that a NiWS phase analogous to the CoMoS phase exists.

Addition of chelating agents such as nitrilotriacetic acid (NTA), ethylenediaminetetraacetic acid (EDTA), and 1,2-cyclohexanediamine-*N*,*N*,*N*′,*N*′-tetraacetic acid (CyDTA) has a beneficial effect on the catalytic activity of CoMo, NiMo, and NiW catalysts, irrespective of the support (14–18, 22, 23). Work in the laboratories of Prins (15–17) and our own group (18–20) has identified retardation of Ni and Co sulfide formation as the key step in enabling the formation of the active NiMoS and CoMoS phases (18–20). Recently Shimizu *et al.* (22) also showed that chelating agents improve the activity in HDS of benzothiophene and in hydrogenation of *o*-xylene over NiW/Al_2O_3 catalysts.

Model catalysts consisting of a flat conducting substrate covered with a thin SiO_2 or Al_2O_3 layer on top of which the active phase is deposited have been proven very useful in catalyst preparation studies (24). The advantage of

---

[1] To whom correspondence should be addressed at P.O. Box 513, 5600 MB Eindhoven, The Netherlands. Fax: 0031 40 245 5054. E-mail: J.W.Niemantsverdriet@tue.nl.

0021-9517/00 $35.00

these model systems, having a conducting substrate, is that sample charging is largely eliminated, resulting in much better resolution of X-ray photoelectron spectra (XPS) with respect to high-surface-area catalysts. To keep the impregnation chemistry identical to that of industrial catalysts, we prepare our model catalysts by spin coating from aqueous solutions on the flat, thin SiO_2 or Al_2O_3 layers, which mimics the conventional pore- volume impregnation used for high-surface-area catalysts (25, 26). These models of hydrotreating catalysts exhibit "realistic" activities and product distributions in thiophene HDS (18–20).

In this article, we investigate the sulfidation behavior of NiW/SiO_2 catalysts prepared without and with various chelating agents and correlate the rate of sulfidation with the activity in thiophene hydrodesulfurization. A preliminary report on the effect of adding CyDTA in the preparation of NiW/SiO_2 model catalysts has been published elsewhere (27).

EXPERIMENTAL

Silica model supports were prepared by oxidizing a Si (100) wafer in air at 750°C for 24 h. The thickness of the amorphous SiO_2 overlayer is estimated as 90 nm and the roughness of the SiO_2 layer is below 1 nm. After calcination the wafers were cleaned in a mixture of H_2O_2 and NH_4OH (3/2 v/v) at 65°C. Subsequently, the surface was hydroxylated by boiling the model supports in water for 30 min, which leads to a hydroxyl population of 4–5 OH groups/nm^2 (28). Next the wafer was covered with a solution of the catalyst precursors and spin-coated under N_2 atmosphere at 2800 rpm (26).

The catalyst precursor compounds were ammonium metatungstate, nickel nitrate ($Ni(NO_3)_2 \cdot 6H_2O$), NTA, EDTA, and CyDTA, all obtained from Merck. The concentration of W and Ni in the precursor solutions was adjusted to result in a loading of 6 W atoms/nm^2 and 2 Ni atoms/nm^2 after spin coating for samples that were used in the XPS studies, whereas for HDS activity studies the Ni loading was varied from 1 to 6 atoms/nm^2. The samples containing NTA, EDTA, and CyDTA were prepared by spin coating with ammonical solutions, which contained the precursors of W, Ni, and NTA (or EDTA or CyDTA) with an atomic ratio of 3 : 1 : 1, such that the amount of chelating agent was equivalent to that of Ni.

After being spin-coated, the catalysts were dried and calcined in a glass reactor under a 20% O_2/Ar gas flow at 1.5 bar. The catalysts were heated to 500°C at a rate of 5°C/min and were kept at the desired temperature for 30 min. Catalysts containing chelating agents (NTA, EDTA, and CyDTA) were used without calcination.

The model catalysts were sulfided in a glass tube reactor with a mixture of 10% H_2S/H_2 at a flow rate of 60 ml/min. The catalysts with chelating agents (NTA, EDTA, and CyDTA) were heated at a rate of 2°C/min (other catalysts at 5°C/min) to the desired temperature and kept there for 30 min. After sulfidation, the reactor was cooled to room temperature under helium gas flow and then brought to a glove-box, where the model catalyst was mounted in a transfer vessel for transport to XPS under N_2 atmosphere.

XPS spectra were obtained by using a VG Escalab 200MK spectrometer equipped with a dual Al/Mg $K\alpha$ X-ray source and a hemispherical analyzer with a five-channel detector. Measurements were recorded with constant pass energy of 20 eV. Binding energies were corrected for charging by using Si 2p peak of SiO_2 at 103.3 eV as a reference. Binding energy values thus determined are estimated to possess an accuracy of ±0.2 eV.

Model catalysts were tested in thiophene HDS (gas phase) to determine the activity and product distribution. Measurements were carried out in a microflow reactor under standard conditions (1.5 bar, 400°C, 4% thiophene/H_2). About 5 cm^2 of model catalyst was placed inside a glass reactor. First, the model catalyst was sulfided at 400°C for 30 min as described above. Then a mixture of 4% thiophene/H_2 was passed through the reactor at a rate of 50 ml/min and at 400°C. After 5 min the reactor was closed and operated as a batch reactor. Although this procedure has the risk that the reaction mixture is insufficiently homogeneous due to lack of mixing, the activities on a per tungsten basis are similar to those measured in flow mode with a high-surface-area catalyst. After the desired reaction time, a sample was taken from the reactor with a calibrated gas tight syringe for gas chromatograph analysis of the reaction products. Then the reactor was flushed with thiophene/H_2 for 5 min and closed again for the next reaction. Blank runs of the empty reactor and bare model support were also performed. The activity of the model catalysts is expressed as the percentage of thiophene converted into products per 5 cm^2 of catalyst and has been corrected for conversion of the empty SiO_2/Si(100) model support (19).

RESULTS

First, we will discuss the state of Ni and W during sulfidation, as determined by XPS. Next we present the results of thiophene HDS and correlate the catalytic activity with the relative sulfidation rates of Ni and W.

Sulfidation of Tungsten in W/SiO_2 and NiW/SiO_2 Catalysts

Figure 1A shows W 4f XPS spectra of the uncalcined NiW/SiO_2 model catalyst after sulfidation in a H_2S/H_2 mixture at different temperatures. It appeared that the sulfidation of W proceeded similarly in W/SiO_2 and in the NiW/SiO_2 catalysts prepared with or without chelating agents. We therefore only discuss the series of W 4f spectra in Fig. 1A.

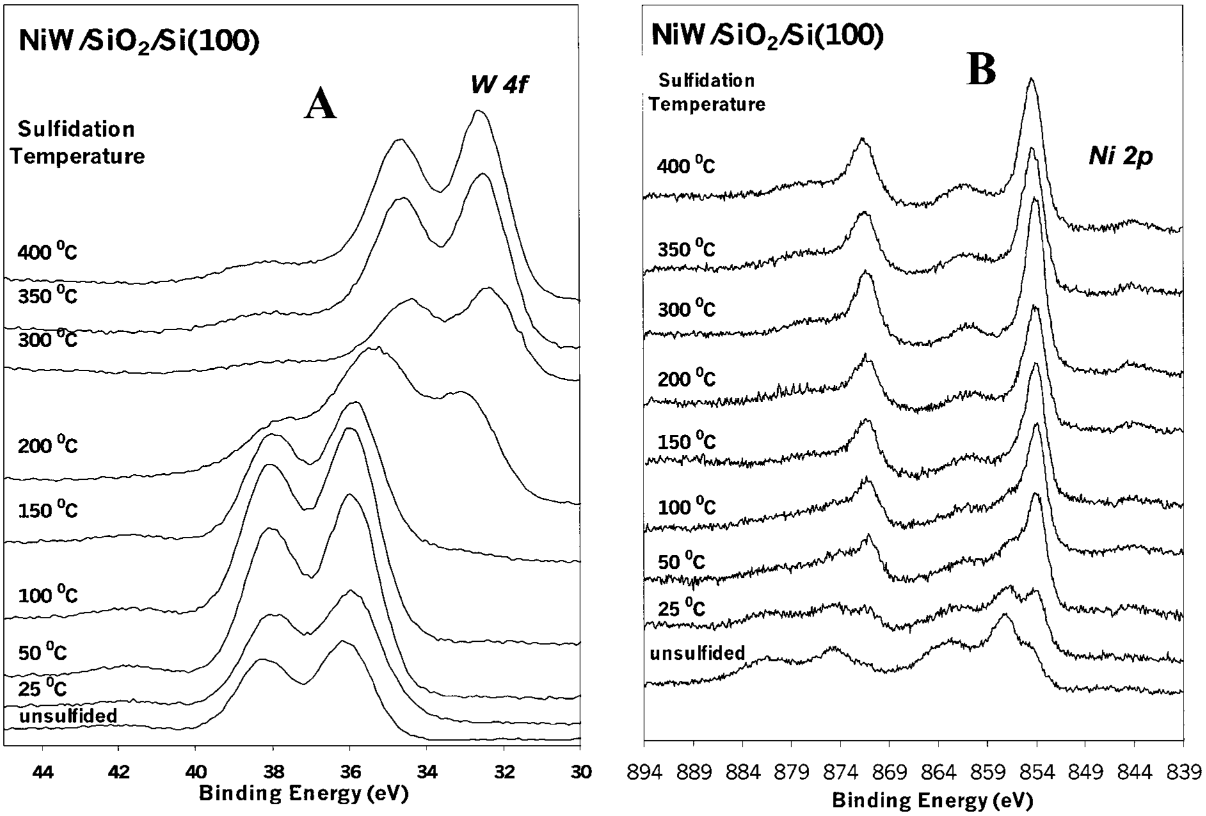

FIG. 1. W 4f (A) and Ni 2p (B) XPS spectra of uncalcined NiW/SiO_2 model catalyst after stepwise sulfidation at various temperatures.

The W 4f spectrum of the unsulfided W/SiO_2 and NiW/SiO_2 catalysts exhibits a doublet with the $4f_{7/2}$ peak at 36.0 ± 0.1 eV, which is characteristic of W-oxide with an oxidation state of 6+ (29). The small peak at 41.9 eV with FWHM of 1.9 eV is assigned to the W $5p_{3/2}$ state. In case chelating agents such as NTA, EDTA, and CyDTA were applied in the preparation, the $4f_{7/2}$ binding energy was about 0.4 eV lower, indicating interaction of W with the complexing agent.

Sulfidation starts to affect the W at about 150°C, as evidenced by the appearance of a shoulder at lower binding energy. Separate studies indicate that this is due to reduction of the W-oxide, without incorporation of sulfur into the structure (30). W-sulfide formation is characterized by the appearance of the W $4f_{7/2}$ peak at 32.6 eV and is completed at temperatures between 300 and 350°C. The spectrum shows a single W 4f doublet at 32.6 eV, characteristic of WS_2 (29). The S 2p spectra of the W/SiO_2 catalyst (not shown) confirm that the sulfidation starts at around 150°C and that the area of S 2p increases with increasing sulfidation temperature. The S 2p spectra can be fitted with a single doublet with S $2p_{3/2}$ binding energy of 161.8 eV, consistent with the S^{2-}-type ligands present in WS_2.

Neither calcination of the catalysts, nor variation of the W loading, nor addition of chelating agents affected the sulfidation rate of tungsten significantly.

Sulfidation of Nickel in Ni/SiO_2 and NiW/SiO_2 Catalysts

Ni/SiO_2. Figure 2A shows the Ni 2p XPS spectra of a calcined Ni/SiO_2 model catalyst recorded after sulfidation at various temperatures. The Ni 2p spectrum of the unsulfided catalyst exhibits a Ni 2p doublet at 856.8 eV and a shake-up feature at higher binding energy, which is a characteristic pattern for nickel oxide with an oxidation state of 3+ (29). A shoulder at 854.9 eV in the spectrum of fresh Ni/SiO_2 points to the presence of hydrated oxide (29), possibly formed when the calcined catalyst was exposed to the ambient atmosphere. The Ni 2p XPS spectrum obtained for the model catalyst, upon sulfidation at room temperature, exhibited an additional doublet at lower binding energy (~854.0 eV). With increasing temperature, the intensity of this additional doublet was found to increase at the expense of the doublet at 856.8 eV, which disappeared completely at ~100°C. The Ni 2p doublet with a binding energy of 854.0 eV measured after sulfidation at higher temperatures corresponds to that of bulk Ni sulfide, Ni_3S_2 (20, 29). The Ni 2p doublet of Ni sulfide also shows shake-up features at higher binding energy, although the intensity of the peaks is less than in the case of oxidic Ni.

The S 2p spectra (not shown) confirm that the sulfidation starts already at room temperature. From the Ni 2p/S 2p intensity ratio it was concluded that the sulfidation of Ni is

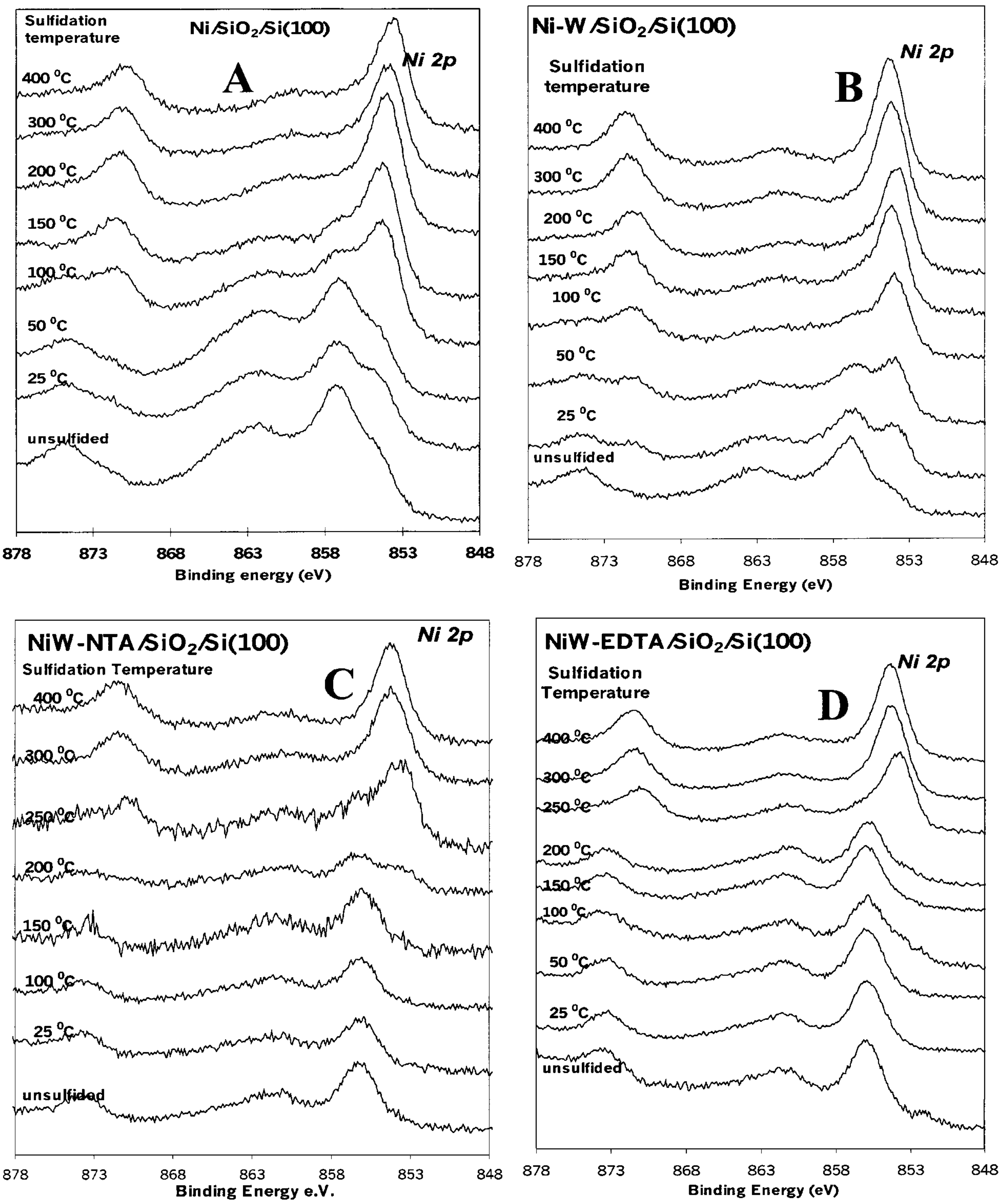

FIG. 2. Ni 2p XPS spectra of (A) Ni/SiO_2, (B) calcined NiW/SiO_2, (C) NiW–NTA/SiO_2, and (D) NiW–EDTA/SiO_2 model catalysts after sulfidation at various temperatures. The spectra show that the presence of complexing agents such as NTA and EDTA retards the sulfidation of Ni at higher temperatures.

TABLE 1

Binding Energies and FWHM of Ni 2p and W 4f XPS Peaks of Fully Oxidic and Sulfidic NiW Model Catalysts

Catalyst	Ni_{ox} $2p_{3/2}$ (eV)	Ni_{Sulf} $2p_{3/2}$ (eV)	W_{ox} $4f_{7/2}$ (eV)	W_{sulf} $4f_{7/2}$ (eV)
Ni/SiO_2	856.8 (3.0)	854.0 (2.4)	—	—
Ni-EDTA/SiO_2	856.1 (2.5)	853.9 (2.5)	—	—
W/SiO_2	—	—	35.9 (1.9)	32.6 (1.6)
NiW/SiO_2	857.1 (2.6) 854.9 (2.1)	854.4 (2.6)	36.1 (1.6)	32.6 (1.7)
NiW/SiO_2 calc.	856.9 (3.2)	854.4 (2.4)	36.0 (1.8)	32.6 (1.7)
NiW-NTA/SiO_2	856.0 (3.1)	854.4 (2.7)	35.6 (2.2)	32.5 (1.8)
NiW-EDTA/SiO_2	856.0 (2.7)	854.5 (2.4)	35.7 (2.2)	32.6 (1.6)
NiW-CyDTA/SiO_2	855.4 (2.4)	854.5 (2.3)	35.6 (2.0)	32.6 (1.6)

complete at temperatures around 100°C. The binding energy of Ni sulfide does not change in the entire sulfidation temperature range (25 to 400°C).

Addition of EDTA to the impregnating solution from which the Ni/SiO_2 is prepared leads to a slower sulfidation of the Ni (not shown). The Ni 2p spectrum of the unsulfided Ni–EDTA catalyst exhibited a pattern characteristic of Ni^{2+} with the Ni 2p doublet at 856.1 eV accompanied by shake-up features at higher binding energy. Hence, the binding energy for Ni–EDTA (856.1 eV) is lower than that observed for the catalysts without EDTA (856.8 eV; see Table 1), providing evidence for complexation of the Ni by the EDTA. Sulfidation of Ni–EDTA/SiO_2 started at temperatures above 200°C, i.e., significantly later than measured for the standard Ni/SiO_2 catalyst discussed above. After completion of the sulfidation at temperatures around 250°C, the Ni $2p_{3/2}$ binding energy of 853.9 eV indicated formation of bulk Ni_3S_2. Similar experiments were performed with Ni–NTA/SiO_2 and Ni–CyDTA/SiO_2 catalysts and gave very similar results although the temperature at which sulfidation begins varies with the ligands in the order NTA < EDTA < CyDTA. However, in all cases, the binding energy of the final Ni sulfide is the same (853.9 ± 0.1 eV).

NiW/SiO_2. Figure 1 shows the Ni 2p XPS spectra together with those of W 4f of the uncalcined silica-supported NiW catalyst with a loading of 6 W atoms/nm^2 and Ni 2 atoms/nm^2 after sulfidation at various temperatures. Peak positions of the oxidic and sulfidic contribution of both the Ni $2p_{3/2}$ and the W $4f_{7/2}$ photoemission lines and degree of sulfidation of both elements upon the various sulfidation temperatures are presented in Table 2. As Fig. 1 and Table 2 show, the sulfidation of W starts at around 150°C and is completed at 350°C, whereas that of Ni starts at room temperature and is finished at 150°C. Hence, sulfidation of Ni 2p and that of W 4f occur in separate temperature regimes.

Calcination of the NiW/SiO_2 catalyst retards the sulfidation of Ni somewhat. The Ni 2p XPS spectra of this catalyst (Fig. 2B) indicate that Ni sulfidation starts at room temperature but converts more slowly to the sulfided state than the uncalcined NiW catalyst does, as is evident if the Ni spectra after reaction at 50°C are compared.

Interestingly, the binding energy of Ni shifts gradually from 854.0 eV after sulfidation at 150°C (characteristic of Ni_3S_2) to 854.4 eV at higher temperatures as W converts to the sulfidic state. Such a shift has not been observed for Ni/SiO_2 with or without chelating agents. We discuss the indication of this shift under Discussion.

Sulfidation of Nickel in NiW/SiO_2 Catalysts Prepared with Chelating Agents

Figures 2C and 2D illustrate the effect of NTA and EDTA on the sulfidation of Ni in NiW/SiO_2 catalysts. Clearly, the effect is to stabilize the Ni such that sulfidation occurs at higher temperatures than observed for either Ni

TABLE 2

The Binding Energy and FWHM of the Oxidic and Sulfidic Contribution of the Ni $2p_{3/2}$ and W $4f_{7/2}$ Emission Lines and Degree of Sulfidation of Both Elements upon the Various Sulfidation Temperature for Uncalcined NiW/SiO_2 Model Catalysts

Sulfidation temperature	Ni $2p_{3/2}$ (eV)			W $4f_{7/2}$ (eV)		
	Oxide	Sulfide	%$Ni_{sulfide}$	Oxide	Sulfide	%$W_{sulfide}$
Unsulfided	857.1 (2.6) 854.9 (2.1)	—	—	36.1 (1.6)	—	—
25°C	856.9 (3.1)	854.0 (2.4)	46	36.0 (1.8)	—	—
50°C	856.6 (3.3)	853.9 (2.2)	55	36.0 (1.7)	—	—
100°C	856.4 (2.9)	853.9 (2.2)	80	36.0 (1.7)	—	—
150°C	—	854.0 (2.5)	100	35.9 (1.7)	33.0 (1.8)	6
200°C	—	854.0 (2.3)	100	35.7 (2.3)	33.0 (2.0)	54
300°C	—	854.2 (2.6)	100	36.0 (2.0)	32.5 (1.7)	91
350°C	—	854.3 (2.6)	100	—	32.6 (1.6)	100
400°C	—	854.4 (2.6)	100	—	32.6 (1.7)	100

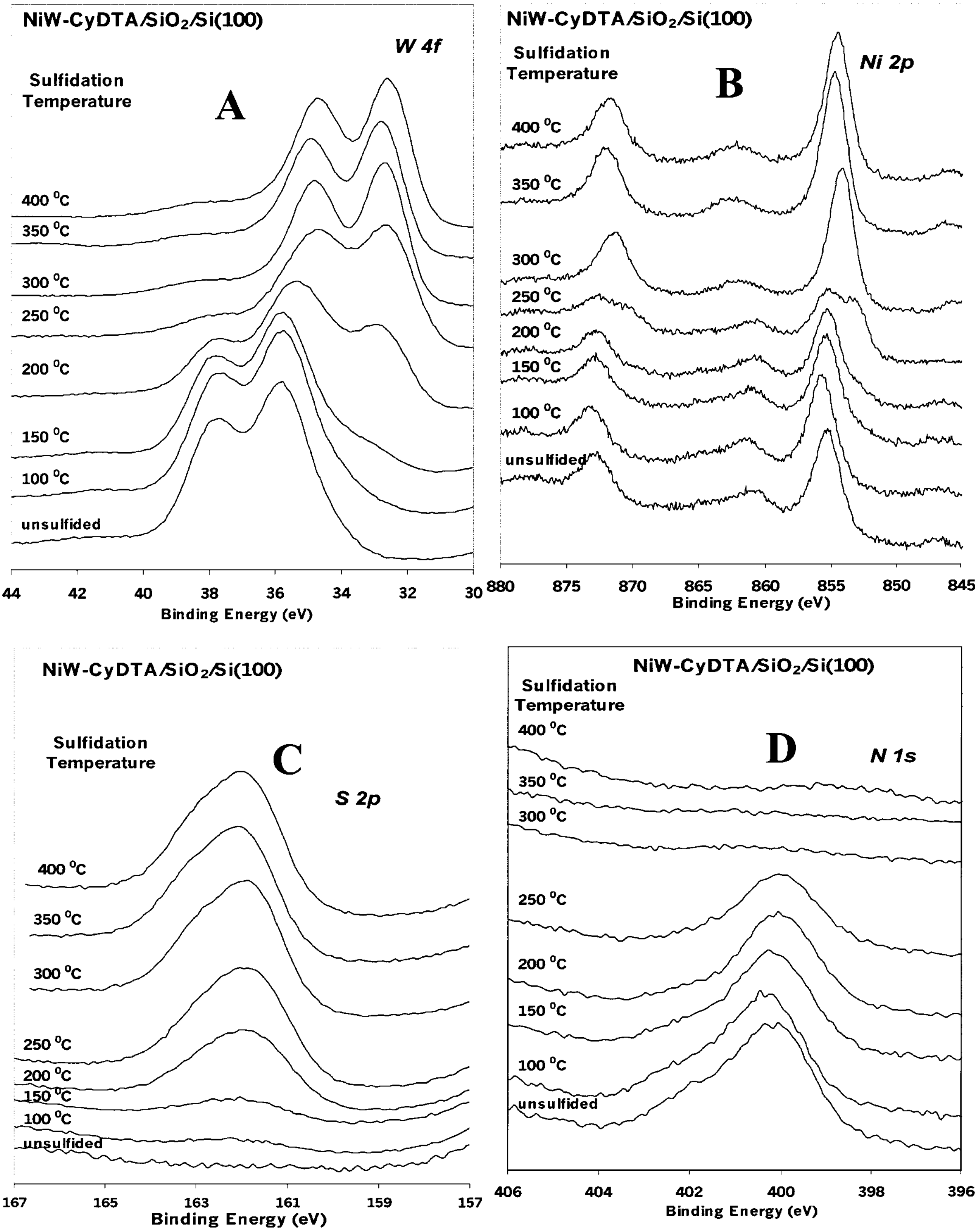

FIG. 3. (A) W 4f, (B) Ni 2p, (C) S 2p, and (D) N 1s XPS spectra of NiW–CyDTA/SiO_2 model catalyst as a function of sulfidation temperature, showing that CyDTA retards the sulfidation of Ni at temperatures where WS_2 has been formed. Ni sulfide formation parallels the disappearance of the N 1s signal, indicating that the decomposition of CyDTA determines the rate of Ni sulfidation.

or NiW/SiO_2 catalysts. The stabilizing effect of EDTA is stronger than that of NTA. We will discuss the effect of the even stronger chelating agent CyDTA in more detail.

Figure 3 shows the evolution of W, Ni, S, and N in the NiW–CyDTA/SiO_2 catalyst during sulfidation in H_2S/H_2. The W 4f spectrum of the unsulfided catalysts in Fig. 3A shows a doublet at 35.6 eV with full width at half-maximum (FWHM) of 2.0, which is characteristic of oxidic W in an oxidation state of 6+ (29). The Ni 2p spectrum of the unsulfided catalyst shows the characteristic pattern of oxidic Ni, however, with an unusually low binding energy of 855.4 eV, which we attribute to complexation with CyDTA. The N 1s peak around 400 eV is characteristic of the CyDTA ligand. The S 2p region shows no emission as expected.

Upon sulfidation, W is the first element to be affected, which occurs around 150°C. The S 2p region shows the appearance of sulfur. Ni, however, is not affected until temperatures of 250°C are reached. Sulfidation of Ni is complete at 300°C. Close inspection of N 1s spectra reveals that the intensity of the nitrogen signal disappears at temperatures above 250°C. Hence, we conclude that sulfidation of Ni is retarded until the Ni–CyDTA complex decomposes. A similar situation occurred in high-surface-area $NiMo/SiO_2$ catalysts prepared with NTA as the chelating complex, as reported in an EXAFS study by Medici and Prins (16).

The conversion from oxidic to sulfidic phases is reflected by the S 2p spectra (Fig. 3C). In the spectra obtained after sulfidation at 150 and 200°C, the signal corresponds to the sulfidic part of W only, whereas from 250°C onward the S 2p peaks have the contribution of both Ni and W sulfide. The S 2p spectra can be fitted with a doublet of S $2p_{3/2}$ binding energy of 161.8 eV, consistent with sulfur with a formal charge of −2 (8, 9).

The results in Fig. 3 clearly show that addition of CyDTA in the preparation completely reverses the order in which Ni and W convert to sulfides (W first, Ni second) compared to the standard NiW/SiO_2 catalyst, where Ni sulfidation precedes that of W.

Comparison Sulfidation of NiW Catalysts

Figure 4 shows the degree of sulfidation of W and Ni for all the catalysts as a function of sulfidation temperature, as derived from the XPS spectra. Sulfidation of W in all catalysts is similar and is indicated by the heavy line in Fig. 4. One clearly observes the retarding effect of calcination and of the chelating agents NTA, EDTA, and CyDTA on the sulfidation of Ni.

Figure 5 shows the Ni $2p_{3/2}$ binding energy of the Ni-sulfide phase versus sulfidation temperature. A nickel-only (Ni/SiO_2) catalyst, which already forms sulfide at room temperature, contains Ni with a binding energy of 854.0 eV, similar to that of bulk Ni_3S_2 irrespective of sulfidation temperature. Also the XPS spectrum of the standard NiW/SiO_2 catalyst exhibits this phase for sulfidation temperatures below 250°C. However, all NiW catalysts sulfided at temperatures of 300°C and higher exhibit a Ni $2p_{3/2}$ binding energy that is significantly, i.e., 0.35–0.50 eV, higher than that of bulk Ni_3S_2 and indicative of a different structure. As this shift in binding energy occurs at the temperatures where WS_2 forms, we believe that WS_2 accommodates the change in Ni sulfide structure.

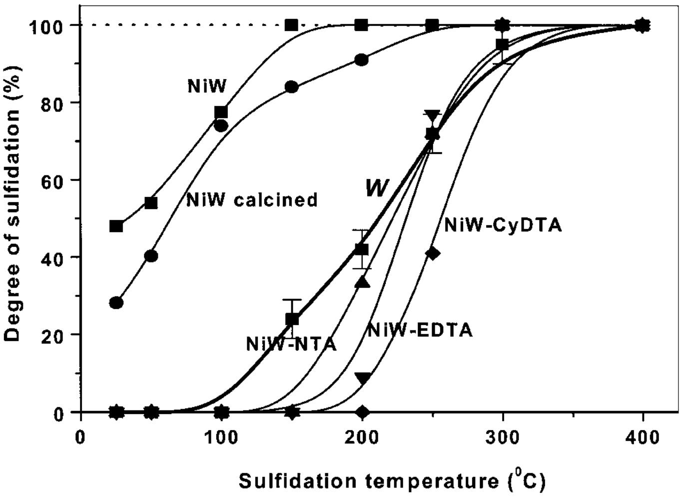

FIG. 4. Degree of sulfidation of Ni and W in various NiW catalysts as a function of sulfidation temperature. Note that complexing agents stabilize Ni against sulfide formation.

Thiophene Hydrodesulfurization

All catalysts were tested on their performance in thiophene HDS. As an example, Fig. 6 shows the yield of the main products and the total conversion of thiophene of the NiW–EDTA/SiO_2 catalyst versus reaction time in a batch

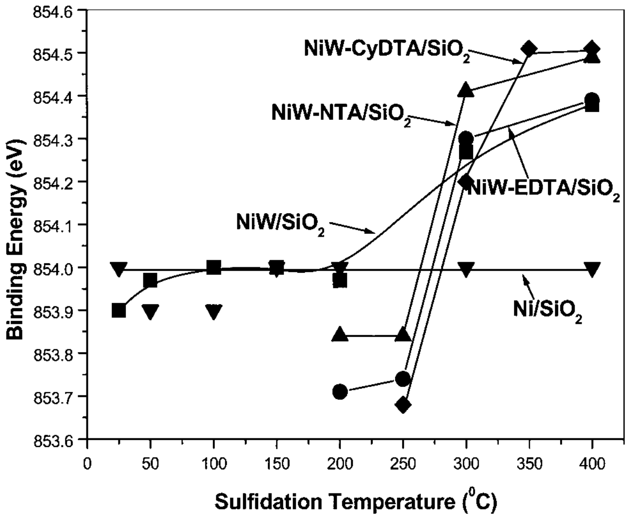

FIG. 5. Ni $2p_{3/2}$ binding energy of Ni sulfide in various catalysts as a function of sulfidation temperature.

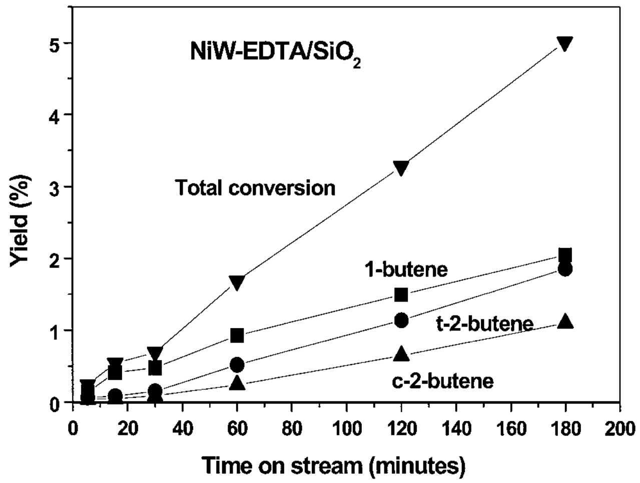

FIG. 6. Thiophene hydrodesulfurization experiment on NiW–EDTA/SiO_2 model catalyst. The loading of Ni and W is 2 and 6 atoms/nm^2, respectively. The figure shows the product yield in a batch reaction at 400°C as a function of reaction time.

experiment. The yields are based on a 5-cm^2 surface area of catalyst and have been corrected for conversion of an empty SiO_2 support in a blank experiment. These blanks showed some conversion of thiophene (0.03%) to mainly methane, ethane, and propane, thought to be due to thermal decomposition of thiophene, which may be assisted by the reactor wall. The product distribution in Fig. 6 shows the most important products, 1-butene, *trans*-2-butene, and *cis*-2-butene. We also observed minor quantities of C_1–C_3 cracking products (not shown). Butane was not observed. The yield of products increases roughly linearly with reaction time, indicating that no significant deactivation occurs. At low conversions the primary product, 1-butene, is the dominant product. As the reaction progresses, the conversion increases and the relative amount of the secondary products, *trans*-2-butene and *cis*-2-butene, increases. At high conversion after a longer reaction time than indicated in Fig. 6, *trans*-2-butene even becomes the main product.

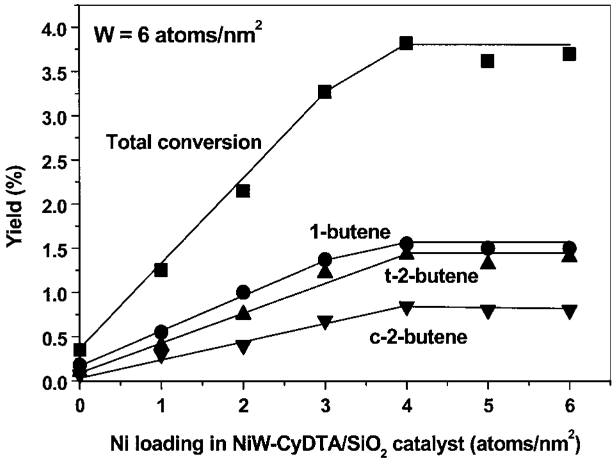

FIG. 7. Product yield of thiophene hydrodesulfurization at 400°C for 1 h in a batch reaction over NiW–CyDTA/SiO_2 model catalysts, as a function of Ni loading, showing that the optimum composition corresponds to a Ni : W ratio of 0.66.

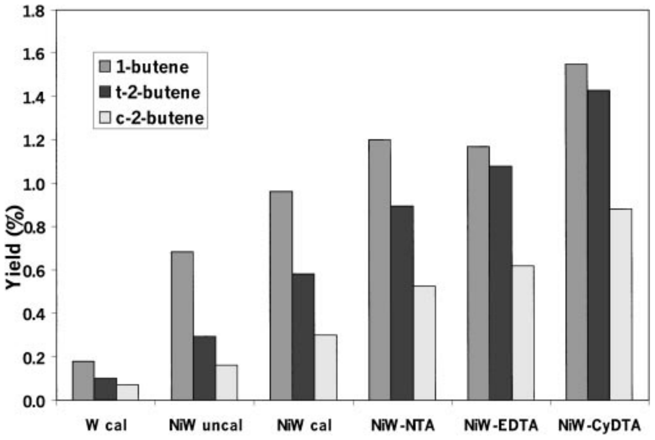

FIG. 8. Thiophene hydrodesulfurization over NiW model catalysts supported on silica prepared in different ways, showing the product distribution after 1 h of batch reaction at 400°C.

Figure 7 illustrates the promoting effect of Ni on the HDS activity of tungsten in NiW–CyDTA/SiO_2 model catalysts. The activity increases with Ni loading until a Ni-W ratio of 0.66 is reached, after which the activity levels off. Interestingly, the optimum Ni : W atomic ratio of 0.66 is equal to that in commercial NiW/Al_2O_3 catalysts (2).

Figure 8 compares the catalytic performance of all the NiW/SiO_2 catalysts with optimum loading of 6 W atoms/nm^2 and 4 Ni atoms/nm^2. The beneficial effect of Ni on W and of the chelating agents on the activity of the NiW/SiO_2 catalysts is evident.

DISCUSSION

Promotion of W by Ni in sulfidic catalysts leads to a significant increase in catalytic activity for the hydrodesulfurization of thiophene to 1- and 2-butene, and the promoting effect becomes significantly higher if chelating agents such as NTA, EDTA, and CyDTA are added in the impregnation stage. The activity increases with increasing Ni : W atomic ratio and reaches a plateau at a ratio of 0.66.

An important conclusion from this work is that a clear correlation exists between the thiophene HDS activity of NiW/SiO_2 catalysts and the order in which the initially oxidic Ni and W convert to the sulfidic state during presulfidation in H_2S/H_2. This becomes immediately apparent if one compares Fig. 8, where the catalytic performance of different NiW/SiO_2 is shown, with Fig. 4, showing the degree of sulfidation of Ni and W versus temperature. There is a one-to-one correspondence between the extent to which sulfidation of nickel is retarded and the activity of the NiWS/SiO_2 catalyst in thiophene HDS.

These findings are readily rationalized if one assumes that the optimum structure of the active phase in a sulfidic NiW/SiO_2 catalyst is the analogue of the well-known CoMoS phase (2, 4, 5, 14, 16, 18, 19, 21), in which sulfidic Ni decorates the edges of WS_2 particles. Retarding the sulfidation of Ni by coordinating it to a sufficiently stable agent such as CyDTA is favorable, because the Ni is released at temperatures where WS_2 has already been formed. Of course, we cannot rule out the possibility that the chelating agents play a beneficial role with respect to the size of the WS_2 particles as well, but we believe that the stabilizing effect on the Ni is the main contributor. The detailed XPS measurements of the NiW–CyDTA/SiO_2 system in Fig. 3 clearly illustrate this point: Ni starts to form sulfides at the temperatures where the complex decomposes, as revealed by the intensity decrease of the N 1s spectra characteristic of the CyDTA complex.

Note that NTA was sufficiently stable to achieve the desired retardation of Co in CoMo (16, 18, 19) and Ni in NiMo (15, 20) catalysts, because Mo forms sulfides at lower temperatures. As W is significantly more difficult to sulfide than Mo, chelating agents more stable than NTA such as EDTA and CyDTA are necessary to achieve the desired effect in NiWS catalysts.

Nonetheless, one cannot state that retardation of Ni sulfidation is the sole determining factor in reaching a high level of activity, as sulfidation of a standard NiW catalyst, in which Ni sulfidation entirely precedes that of W, shows significant HDS activity as well and significantly higher than that of a single WS_2/SiO_2 catalyst. The Ni 2p XPS spectra of this catalyst give a hint why this is so: As Fig. 5 shows, the binding energy of Ni in partially sulfided NiW/SiO_2 increases from 854.0 eV, the value of Ni_3S_2, to 854.4 eV, the value corresponding to the active state of the catalyst, at the temperatures where WS_2 formation is complete. This strongly suggests that the Ni_3S_2 formed at low temperatures rearranges at higher temperatures. Interpreted in terms of the CoMoS structure, it is likely that the nickel redisperses over the edges of the WS_2 crystallites, as proposed earlier by Reinhoudt *et al.* (11).

Finally, we note that all results reported here were obtained with planar, conducting model catalysts, exposing typically 5 cm^2 of surface area in the catalytic reaction. The great advantage of using these models is that their XPS spectra feature much better resolution than the spectra of high-surface-area catalysts, which is particularly useful in the case of W where the W 4f doublet splitting is small.

CONCLUSIONS

For a series of differently prepared NiW supported on SiO_2 model catalysts, the rates of sulfidation have been measured by XPS and compared with the activity in thiophene HDS.

- Ni/SiO_2 catalyst forms bulk nickel sulfide in H_2S/H_2 at relatively low temperatures; this catalyst is largely inactive in thiophene HDS.
- W/SiO_2 converts to WS_2 at significantly higher temperatures (150–350°C); this phase shows significant activity for the HDS of thiophene at 400°C.
- In NiW/SiO_2 catalysts prepared by conventional impregnation, Ni converts more rapidly to the sulfidic state before the W starts. However, the Ni_3S_2 phase formed at low temperatures restructures at temperatures where WS_2 has formed; the resulting NiWS phase is about four times more active for thiophene HDS than WS_2.
- Optimum promotion of WS_2 by Ni is observed for Ni : W atomic ratios of 0.66. Higher Ni content does not lead to higher activity.
- Complexing to Ni with chelating agents like NTA or EDTA retards the sulfidation of Ni to higher temperatures, such that both Ni and W form sulfides in the same temperature range. This leads to higher HDS activity than measured from the standard NiW/SiO_2 catalyst.
- Complexing Ni with CyDTA retards the sulfidation of Ni where WS_2 has already formed. Nickel sulfidation starts when the CyDTA complex decomposes. As a result, nickel atoms released by the chelating agent can move to the reactive edges of the WS_2 to form a finely dispersed sulfide. This gives the highest activity for thiophene HDS.

ACKNOWLEDGMENTS

This work has been performed under the auspices of NIOK, The Netherlands Institute for Catalysis Research, with financial support from the Chemical Science Division of The Netherlands Organization for Scientific Research (NWO-CW) and The Netherlands Technology Foundation (STW).

REFERENCES

1. Gosselink, J. W., *CatTech* **4**, 127 (1998).
2. Topsøe, H., Clausen, B. S., and Massoth, F. E., "Hydrotreating Catalysis." Springer-Verlag, Berlin, 1996.
3. Scheffer, B., Mangnus, P. J., and Moulijn, J. A., *J. Catal.* **121**, 18 (1990).
4. Prins, R., De Beer, V. H. J., and Somorjai, G. A., *Catal. Rev. Sci. Eng.* **31**, 1 (1989).
5. Topsøe, H., and Clausen, B. S., *Catal. Rev. Sci. Eng.* **26**, 395 (1984).
6. De Jong, A. M., Borg, H. J., Van IJzendoorn, L. J., Soudant, V. G. M. F., De Beer, V. H. J., Van Veen, J. A. R., and Niemantsverdriet, J. W., *J. Phys. Chem.* **97**, 6477 (1993).
7. Muijsers, J. C., Weber, Th., Van Hardeveld, R. M., Zandbergen, H. W., and Niemantsverdriet, J. W., *J. Catal.* **157**, 698 (1995).
8. Weber, Th., Muijsers, J. C., and Niemantsverdriet, J. W., *J. Phys. Chem.* **99**, 9194 (1995).
9. Weber, Th., Muijsers, J. C., Van Wolput, J. H. M. C., Verhagen, C. P. J., and Niemantsverdriet, J. W., *J. Phys. Chem.* **100**, 14144 (1996).
10. Reinhoudt, H. R., Van Langeveld, A. D., Kooyman, P. J., Stockman, R. M., Prins, R., Zandbergen H. W., and Moulijn, J. A., *J. Catal.* **179**, 443 (1998).

11. Reinhoudt, H. R., Van der Meer, Y., Van der Kraan, A. M., Van Langeveld, A. D., and Moulijn, J. A., *Fuel. Proc. Tech.* **61**, 43 (1999).
12. Breysse, M., Cattenot, M., Decamp, T., Frety, R., Gachet, C., Lacroix, M., Leclerq, C., Mourques, L. de, Portefaix, J. L., Vrinat, M., Houari, M., Grimblot, J., Kasztelan, S., Bonnelle, J. P., Housni, S., Bachelier, J., and Duchet, J. C., *Catal. Today* **4**, 39 (1988).
13. Reinhoudt, H. R., Van Langeveld, A. D., Mariscal, R., De Beer, V. H. J., Van Veen, J. A. R., Sie, S. T., and Moulijn, J. A., *Stud. Surf. Sci. Catal.* **106**, 263 (1997).
14. Van Veen, J. A. R., Gerkema, E., Van der Kraan, A. M., and Knoester, A., *J. Chem. Soc. Chem. Commun.* **22**, 1684 (1987).
15. Cattaneo, R., Shido, T., and Prins, R., *J. Catal.* **185**, 199 (1999).
16. Medici, L., and Prins, R., *J. Catal.* **163**, 38 (1996).
17. Cattaneo, R., Weber, Th., Shido, T., and Prins, R., *J. Catal.* **191**, 225 (2000).
18. De Jong, A. M., De Beer, V. H. J., Van Veen, J. A. R., and Niemantsverdriet, J. W., *J. Phys. Chem.* **100**, 17722 (1996).
19. Coulier, L., De Beer, V. H. J., Van Veen, J. A. R., and Niemantsverdriet, J. W., *Top. Catal.* **13**, 99 (2000).
20. Coulier, L., Beek, W., De Beer, V. H. J., Van Veen, J. A. R., and Niemantsverdriet, J. W., Submitted for publication.
21. Louwers, S. P. A., and Prins, R., *J. Catal.* **139**, 525 (1993).
22. Shimizu, T., Hiroshima, K., Honma, T., Mochizuki, T., and Yamada, M., *Catal. Today* **45**, 271 (1998).
23. Ohta, Y., Shimizu, T., Honma, T., and Yamada, M., *Stud. Surf. Sci. Catal.* **127**, 161 (1999).
24. Gunter, P. L. J., Niemantsverdriet, J. W., Ribeiro, F. H., and Somorjai, G. A., *Catal. Rev. Sci. Eng.* **39**, 77 (1997).
25. Kuipers, E. W., Laszlo, C., and Wieldraaijer, W., *Catal. Lett.* **17**, 71 (1993).
26. Van Hardeveld, R. M., Gunter, P. L. J., Van IJzendoorn, L. J., Wieldraaijer, W., Kuipers, E. W., and Niemantsverdriet, J. W., *Appl. Surf. Sci.* **84**, 339 (1995).
27. Kishan, G., Coulier, L., De Beer, V. H. J., Van Veen, J. A. R., and Niemantsverdriet, J. W., *J. Chem. Soc. Chem. Commun.*, 1103 (2000).
28. Thüne, P. C., Verhagen, C. P. J., Van den Boer, M. J. G., and Niemantsverdriet, J. W., *J. Phys. Chem.* **101**, 8559 (1997).
29. Moulder, J. F., Stickle, W. F., Sobol, P. E., and Bomben, K. D., “Handbook of XPS.” Perkin Elmer, Eden Prairie, MN, 1992.
30. Van der Vlies, A., and Weber, Th., personal communication.